Supplementary Information

High-pressure annealing driven nanocrystal formation in $Zr_{50}Cu_{40}Al_{10}$ metallic glass and strength increase

Yuki Shibazaki[1,*], Rui Yamada[2], Junji Saida[2], Yoshio Kono[3,4], Masato Wakeda[5], Keiji Itoh[6], Masahiko Nishijima[7], Koji Kimoto[8]

[1]International Center for Young Scientists, National Institute for Materials Science, 1-1 Namiki, Tsukuba, Ibaraki, 305-0044, Japan.

[2]Frontier Research Institute for Interdisciplinary Sciences, Tohoku University, 6-3 Aoba, Aramaki, Aoba-ku, Sendai 980-8578, Japan.

[3]Geophysical Laboratory, Carnegie Institution of Washington, 9700 S. Cass Ave., Argonne, Illinois 60439, USA.

[4]Geodynamics Research Center, Ehime University, 2-5 Bunkyo-cho, Matsuyama, Ehime, 790-8577, Japan.

[5]Research Center for Structural Materials, National Institute for Materials Science, 1-2-1 Sengen, Tsukuba, Ibaraki, 305-0047, Japan.

[6]Graduate School of Education, Okayama University, 3-1-1 Tsushima-Naka, Kita-ku, Okayama 700-8530, Japan.

[7]The Electron Microscopy Center, Tohoku University, 2-1-1 Katahira, Aoba-ku, Sendai 980-8577, Japan.

[8]Electron Microscopy Group, Research Center for Advanced Measurement and Characterization, National Institute for Materials Science, 1-1 Namiki, Tsukuba 305-0044, Japan.

[*]Now at Institute of Materials Structure Science, High Energy Accelerator Research Organization (KEK), 1-1 Oho, Tsukuba 305-0801, Japan.

Corresponding authors:

Yuki Shibazaki

E-mail: yuki.shibazaki@kek.jp

Tel: +81-29-864-5200 (ext. 4914)

I. Total structure factors $S(Q)$ obtained by the RMC modeling.

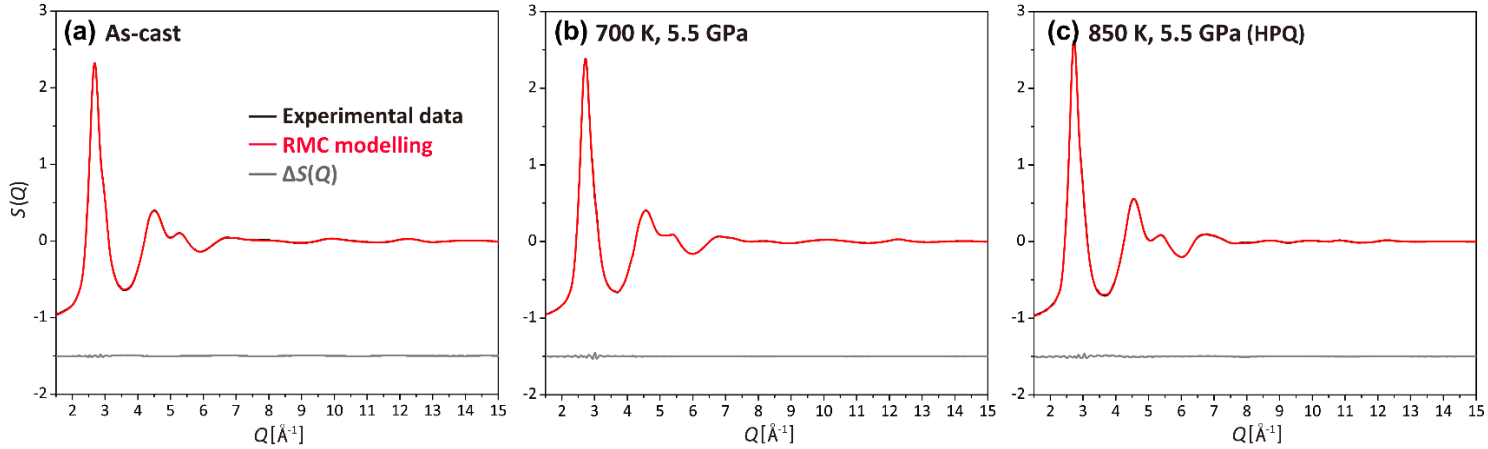

Supplementary Figure 1. Comparisons of structure factors $S(Q)$ between experimental data and RMC modeling for the as-cast sample **(a)**, the sample synthesized at 700 K and 5.5 GPa [$S(Q)$ was obtained at 300 K and 5.5 GPa] **(b)**, and the sample synthesized at 850 K and 5.5 GPa (the HPQ glass) [$S(Q)$ was obtained at 300 K and 5.5 GPa] **(c)**. Black and red curves denote the experimental data and RMC modeling, respectively. Gray curves denote the difference between the experimental data and RMC modeling and are shifted by -1.5 for clarity.

II. Differences of reduced pair distribution function $G(r)$ between samples at high temperature and low temperature for the experimental data and MD simulation.

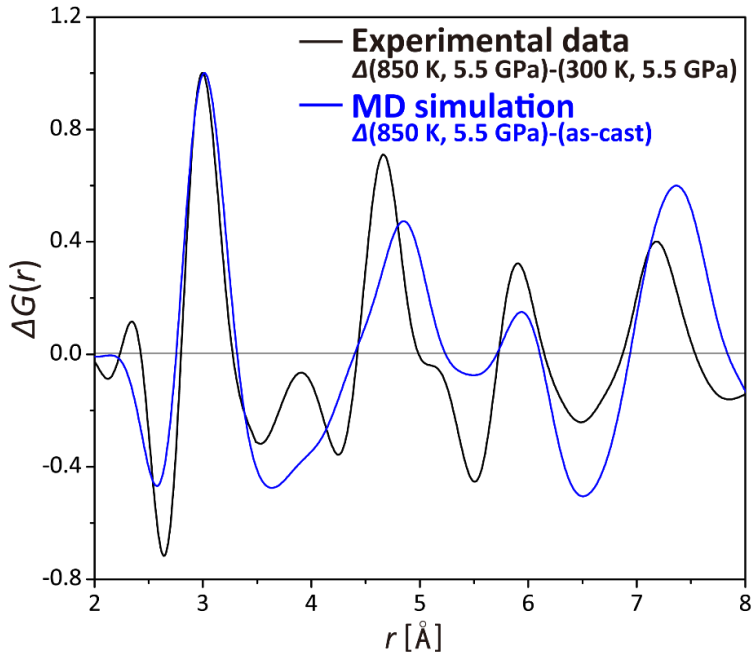

Supplementary Figure 2. $\Delta G(r)$ for the experimental data (black curve) is the difference of $G(r)$ between the samples treated at 850 K and 300 K at 5.5 GPa. $\Delta G(r)$ for MD simulation (blue curve) is the difference of $G(r)$ between the sample treated at 850 K and 5.5 GPa and the as-cast sample. $G(r)$ of the experimental data were collected at 300 K and 5.5 GPa after the heating treatment at the target temperature (850 K or 300 K) at 5.5 GPa, while $G(r)$ of MD simulation were states at 300 K and 0 GPa after the high-pressure heating treatment. Intensities of $\Delta G(r)$ were normalized by each first peak intensity around 3 Å. The intense peak positions for MD simulation, ~3, ~4.7, ~5.9, and ~7.2 Å,

55 are very close to those for the experimental data, implying that the structure changes at
56 high pressure and high temperature observed by MD simulation are in agreement with
57 the experimental results. The peak-top positions for the experimental data slightly shift to
58 lower *r* value because of collecting the data at 5.5 GPa.
59

III. Partial pair distribution functions $g_{ij}(r)$ obtained by the RMC modeling and MD simulation.

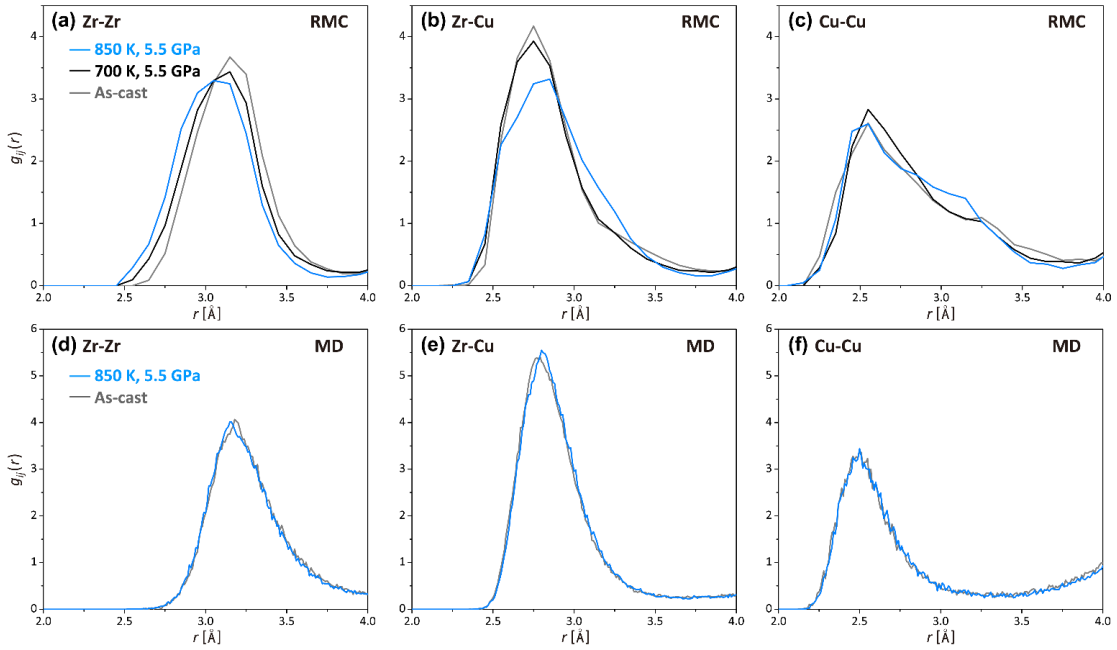

Supplementary Figure 3. Partial pair distribution functions $g_{ij}(r)$ involving Zr–Zr **(a)**, Zr–Cu **(b)**, and Cu–Cu **(c)** correlations obtained by the RMC modeling and those **(d-f)** obtained by the MD simulation. Gray, black, and blue curves denote the $g_{ij}(r)$ for the as-cast sample, the sample synthesized at 700 K and 5.5 GPa, and the sample synthesized at 850 K and 5.5 GPa, respectively.

IV. Cavities in the samples obtained by the RMC modeling.

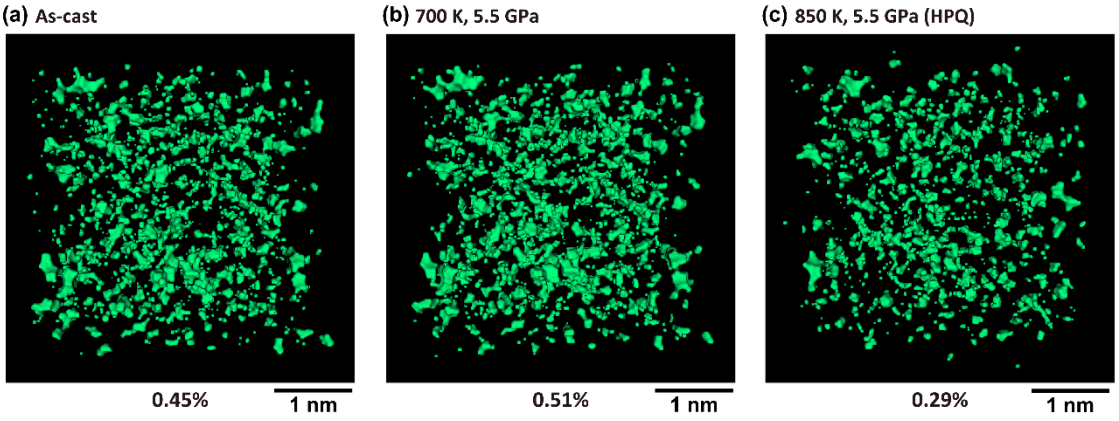

Supplementary Figure 4. Cavities in the as-cast sample **(a)**, the sample synthesized at 700 K and 5.5 GPa **(b)**, and the sample synthesized at 850 K and 5.5 GPa (the HPQ glass) **(c)**. Green region denotes the cavities. Numbers at the bottom are the volume fraction of the cavities. The atoms are not shown.

Distributions of cavities in the samples were calculated by the software pyMolDyn[43] using the atomic configurations obtained by the RMC modeling. The calculation resolution was set to be 256 × 256 × 256 in the cubic box with length of a side of 42.0 Å. Volume fractions of cavities in the samples are 0.45% (as-cast), 0.51% (700 K and 5.5 GPa), and 0.29% (850 K and 5.5 GPa, HPQ), respectively. The volume fraction of cavities drops after the change to the HPQ glass, indicating the dense packing structure of the HPQ glass.

V. Changes in coordination numbers and Cargill-Spaepen short-range order parameters at high pressure and high temperature obtained by the RMC modeling and MD simulation.

Supplementary Table 1. Coordination numbers (CN) and Cargill-Spaepen short-range order parameters (η) in RMC modeling and MD simulation.

	RMC				MD	
	As-cast	5.5 GPa, 700 K	5.5 GPa, 850 K		As-cast	5.5 GPa, 850 K
CN_{Zr}	13.5	13.5	13.5		15.0	14.9
CN_{Cu}	12.9	12.8	12.8		10.7	10.8
CN_{ZrZr}	6.9	6.9	6.7		8.0	7.6
CN_{ZrCu}	5.3	5.5	5.5		5.5	5.8
CN_{CuCu}	5.0	4.9	4.7		2.9	2.7
CN_{CuZr}	6.7	6.6	6.8		6.8	7.2
η_{ZrCu}	0.007	0.006	0.042		0.109	0.158
η_{ZrZr}	-0.005	-0.005	-0.032		-0.063	-0.094
η_{CuCu}	-0.009	-0.008	-0.055		-0.189	-0.268

VI. Typical X-ray diffraction patterns of synthesized samples obtained by a Cu K_α X-ray diffractometer.

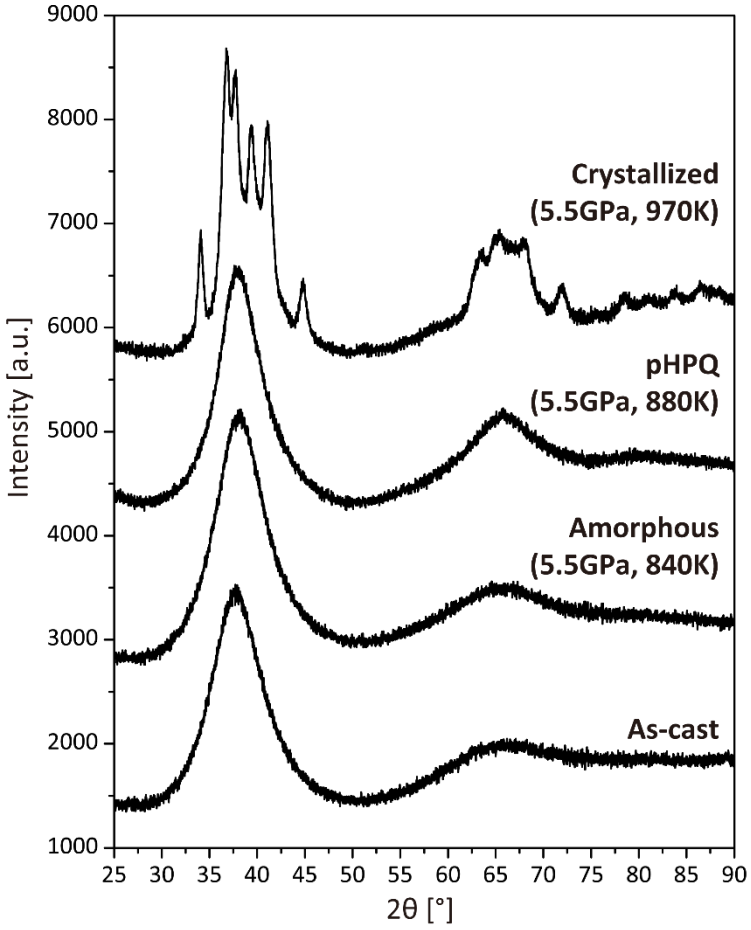

Supplementary Figure 5. A sample was classified as a crystallized sample if sharp X-ray diffraction peaks were observed and as a pHPQ sample if the intensities of the broad first and second peaks increased without sharp peaks. Pressure and temperature values in brackets are synthesized conditions. The data are shifted by 1500 for clarity.

VII. Cell design used in the synchrotron X-ray diffraction experiments.

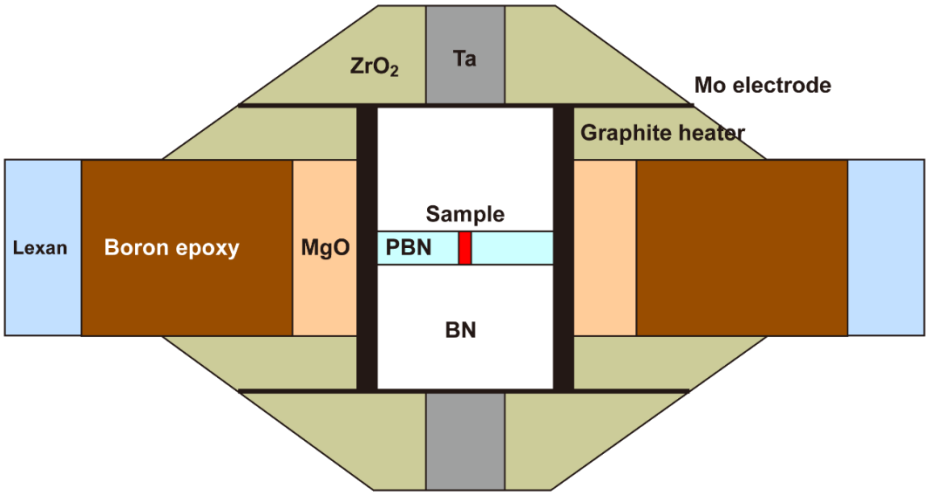

Supplementary Figure 6. We slightly modified the cell assembly of Kono *et al.*[36]. We used pyrolytic BN (PBN) as the X-ray pass inside the BN capsule to minimize the diffraction peaks from the BN capsule in the XRD measurement.

Supplemental Reference

43. Heimbach, I., Rhiem, F., Beule, F., Knodt, D., Heinen, J., & Jones, R. O. pyMolDyn: Identification, structure, and properties of cavities/vacancies in condensed matter and molecules. *J. Comput. Chem*. **38**, 389–394 (2017).